

2 **Environmental controls on drainage behavior of an ephemeral**  
3 **stream**

4 **Kyle W. Blasch · Ty P. A. Ferré · Jasper A. Vrugt**

5  
6 © U.S. Government 2010

7 **Abstract** Streambed drainage was measured at the  
8 cessation of 26 ephemeral streamflow events in Rillito  
9 Creek, Tucson, Arizona from August 2000 to June 2002  
10 using buried time domain reflectometry (TDR) probes. An  
11 unusual drainage response was identified, which was char-  
12 acterized by sharp drainage from saturation to near field  
13 capacity at each depth with an increased delay between  
14 depths. We simulated the drainage response using a variably  
15 saturated numerical flow model representing a two-layer  
16 system with a high permeability layer overlying a lower  
17 permeability layer. Both the observed data and the numerical  
18 simulation show a strong correlation between the drainage  
19 velocity and the temperature of the stream water. A linear  
20 combination of temperature and the no-flow period preced-  
21 ing flow explained about 90% of the measured variations in  
22 drainage velocity. Evaluation of this correlative relationship  
23 with the one-dimensional numerical flow model showed that  
24 the observed temperature fluctuations could not reproduce  
25 the magnitude of variation in the observed drainage velocity.  
26 Instead, the model results indicated that flow duration exerts  
27 the most control on drainage velocity, with the drainage

velocity decreasing nonlinearly with increasing flow dura- 28  
tion. These findings suggest flow duration is a primary 29  
control of water availability for plant uptake in near surface 30  
sediments of an ephemeral stream, an important finding for 31  
estimating the ecological risk of natural or engineered 32  
changes to streamflow patterns. Correlative analyses of soil 33  
moisture data, although easy and widely used, can result in 34  
erroneous conclusions of hydrologic cause—effect rela- 35  
tionships, and demonstrating the need for joint physically- 36  
based numerical modeling and data synthesis for hypothesis 37  
testing to support quantitative risk analysis. 38  
39

**Keywords** Ephemeral stream · Redistribution · 40  
Drainage · Rhizosphere · Restoration 41

**1 Introduction** 42

Many ephemeral stream channels in arid and semi-arid 43  
climates are characterized by relatively short periods of 44  
flow followed by longer no-flow periods (Stonestrom et al. 45  
2007). The magnitude, frequency, duration, and fluvial 46  
geomorphic processes associated with these periods of flow 47  
have been used to describe the suitability of ephemeral 48  
stream channels to support riparian vegetation (Hupp and 49  
Osterkamp 1996; Bendix and Hupp 2000; Lytle and Poff 50  
2004; Shaw and Cooper 2008). Additionally, the impor- 51  
tance of streambed sediments to retain and redistribute 52  
water within the rhizosphere during periods of no-flow has 53  
been identified (Shaw and Cooper 2008). However, the 54  
emphasis has been placed on the cumulative infiltration 55  
prior to cessation of streamflow and evapotranspiration 56  
during cessation (Loik et al. 2001). 57

To date, there have been no published studies describing 58  
environmental controls on the rate of vertical drainage 59

---

K. W. Blasch (✉)  
U.S. Geological Survey, 520 North Park Ave., Suite 221,  
Tucson, AZ 85719, USA  
e-mail: kblasch@usgs.gov

K. W. Blasch · T. P. A. Ferré  
Department of Hydrology and Water Resources, University  
of Arizona, J.W. Harshbarger 122, 1133 East North Campus  
Drive, P.O. Box 210011, Tucson, AZ 85721, USA

J. A. Vrugt  
Earth and Environmental Sciences Division (EES-16),  
Theoretical Division (T-5), Los Alamos National Laboratory,  
Center for Nonlinear Studies (CNLS), Los Alamos,  
NM 87545, USA

|     |  |  |     |
|-----|--|--|-----|
| 60  | through streambed sediments after the cessation of an        | for combining the strengths of quantitative, physically-             | 113 |
| 61  | ephemeral streamflow event. Maximum potential evapo-         | -based modeling and data synthesis to better test scientific         | 114 |
| 62  | transpiration only occurs when the surface and rooting       | hypotheses, by directly comparing correlative and physi-             | 115 |
| 63  | zone are wet. Therefore, streambed drainage rates directly   | cally-based model analyses.  | 116 |
| 64  | influence both cumulative evaporative loss and ground-       |  |     |
| 65  | water recharge beneath channels.                             |  |     |
| 66  | This investigation considered the following environ-         | 1.1 Field methods  | 117 |
| 67  | mental controls on drainage rates: temperature; stage;       |  |     |
| 68  | duration; no-flow duration; and antecedent bed sediment      | 1.1.1 Site description   | 118 |
| 69  | water content. The impact of temperature variability on      |  |     |
| 70  | hydraulic conductivity and streambed infiltration has been   | Rillito Creek is an ephemeral stream in southern Arizona             | 119 |
| 71  | well studied (Constantz 1998; Blasch 2003). Higher sedi-     | that has a drainage area of approximately 2,256 km <sup>2</sup>      | 120 |
| 72  | ment and water temperatures produce higher hydraulic         | (Fig. 1). The channel cross-sectional width at the study site        | 121 |
| 73  | conductivities, which were hypothesized to increase          | is about 75 m. Sediments at the Dodge Boulevard study                | 122 |
| 74  | drainage rates. The influence of temperature, however,       | site consist of an upper layer of recent alluvial stream-            | 123 |
| 75  | decreases with depth as heat is exchanged with the sedi-     | channel deposits and a second deeper layer of Pleistocene            | 124 |
| 76  | ments as water is transported downward. Stage is directly    | or older basin-fill deposits (Davidson 1973). Cores col-             | 125 |
| 77  | proportional to infiltration rate and depth of infiltration  | lected near the site indicate that the alluvial deposits are         | 126 |
| 78  | during an event. The depth of water infiltration into the    | about 7 m thick and consist predominantly of loose to                | 127 |
| 79  | sediments was considered a possible factor controlling       | moderately compacted sands and gravels, with less than 10            | 128 |
| 80  | succeeding drainage. Specifically, higher infiltration rates | percent clay and silt (Hoffmann et al. 2002). The under-             | 129 |
| 81  | would result in a larger volume of water transported into    | lying basin-fill deposits, which extend to depths of several         | 130 |
| 82  | the soil profile and a smaller capillary gradient from the   | hundred meters, consist of unconsolidated to poorly con-             | 131 |
| 83  | ground surface across the wetting front. Likewise, flow      | solidated interbedded gravel, sand, and silt (Davidson               | 132 |
| 84  | duration was thought to increase the depth of infiltration,  | 1973; Hoffmann et al. 2002). The hydraulic properties of             | 133 |
| 85  | and decrease capillary gradients. The decreased gradients    | these layers, estimated on the basis of core data, are listed        | 134 |
| 86  | would reduce drainage rates. No-flow duration defined as     | in Table 1. The water table depth is approximately 40 m at           | 135 |
| 87  | the time period between the cessation of one event and the   | the study site.  | 136 |
| 88  | onset of a succeeding event was considered important as a    | Rillito Creek has two primary seasons of streamflow in               | 137 |
| 89  | surrogate measurement for antecedent conditions of the       | response to two precipitation periods: North American                | 138 |
| 90  | channel sediments. The longer the period of no-flow the      | Monsoon (July–September) and winter (December–                       | 139 |
| 91  | drier the sediment profile becomes caused by evapotrans-     | March). Summer flows typically result from localized,                | 140 |
| 92  | piration at the surface and drainage/dewatering at depth.    | short-duration convective storms, whereas longer-duration            | 141 |
| 93  | Lower antecedent water content at the surface with higher    | frontal storms and snowmelt produce winter flows. During             | 142 |
| 94  | sorptivity was hypothesized to increase the wetting front    | the months of October and November, precipitation from               | 143 |
| 95  | depth. While sediment texture is an important factor to      | tropical storms or changes in weather patterns caused by             | 144 |
| 96  | consider for drainage behavior (coarse sediments have        | periodic climate fluctuations can cause periods of stream-           | 145 |
| 97  | higher conductivities than fine sediments), it was constant  | flow. These events, however, are less common than summer             | 146 |
| 98  | during the study and was thus not considered as a factor for | and winter events. A U.S. Geological Survey (USGS)                   | 147 |
| 99  | the changes in observed drainage rates.                      | streamflow-gaging station, 09485700, is 45 m downstream              | 148 |
| 100 | We present a study of the drainage response of an allu-      | from the study site. Discharge events rarely (<5%) exceed            | 149 |
| 101 | vial stream channel, Rillito Creek, located in Tucson, Ari-  | 28 m <sup>3</sup> /s; the maximum discharge recorded at the site was | 150 |
| 102 | zona (Fig. 1). The study is supported by a large data set    | about 680 m <sup>3</sup> /s during the 1993 El Niño season (Tadayon  | 151 |
| 103 | including soil moisture and temperature measurements at      | et al. 2001).  | 152 |
| 104 | seven depths within the upper 2.5 m collected every 2 min    |  |     |
| 105 | during 26 flow events from August 2000 to June 2002          | 1.1.2 Field measurements   | 153 |
| 106 | (Blasch 2003). From these soil moisture data, we could also  |  |     |
| 107 | infer the duration of flow events, the duration of no-flow   | A 1.5-m wide by 10-m long by 2.5-m deep trench was                   | 154 |
| 108 | periods, and the antecedent soil moisture in the shallow     | excavated perpendicular to the longitudinal axis of the              | 155 |
| 109 | subsurface at the onset of flow.                             | channel. Seven nested pairs of thermocouples and time-               | 156 |
| 110 | In addition to examining drainage responses of ephemer-      | domain reflectometry (TDR) probes were installed in four             | 157 |
| 111 | al streams and their importance for management of            | profiles along the upstream wall of the trench (Fig. 1).             | 158 |
| 112 | riparian areas, the present work demonstrates a clear need   | Once instrumentation was installed, the trench was back-             | 159 |
|     |  | filled. The shallowest sensor depth was 0.5 m; but three             | 160 |

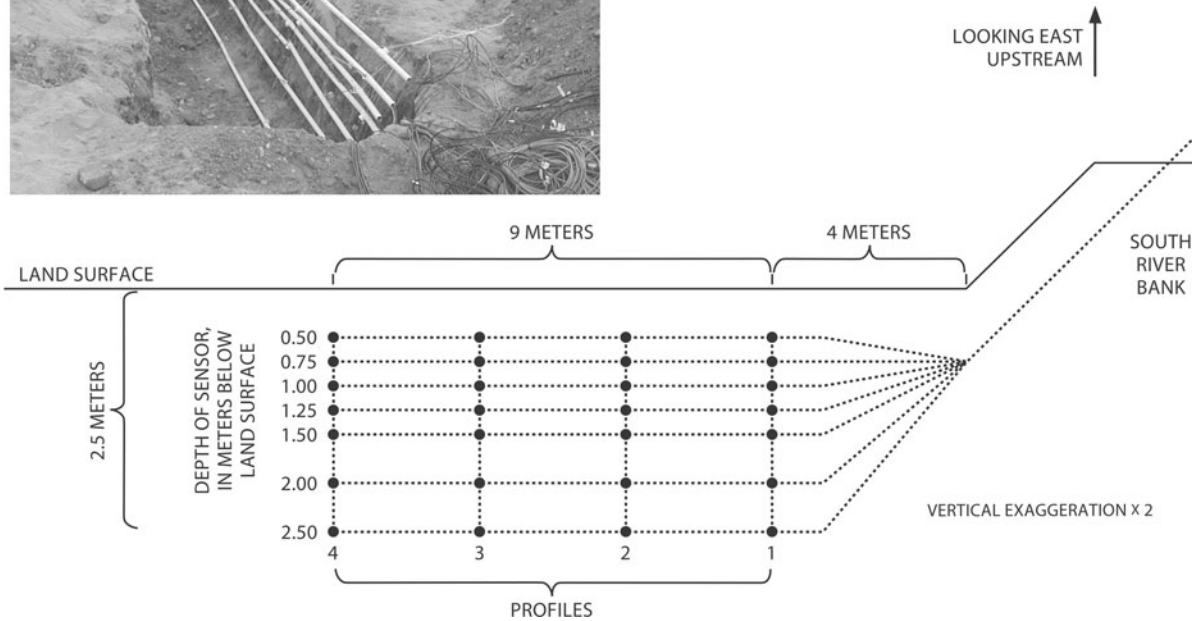
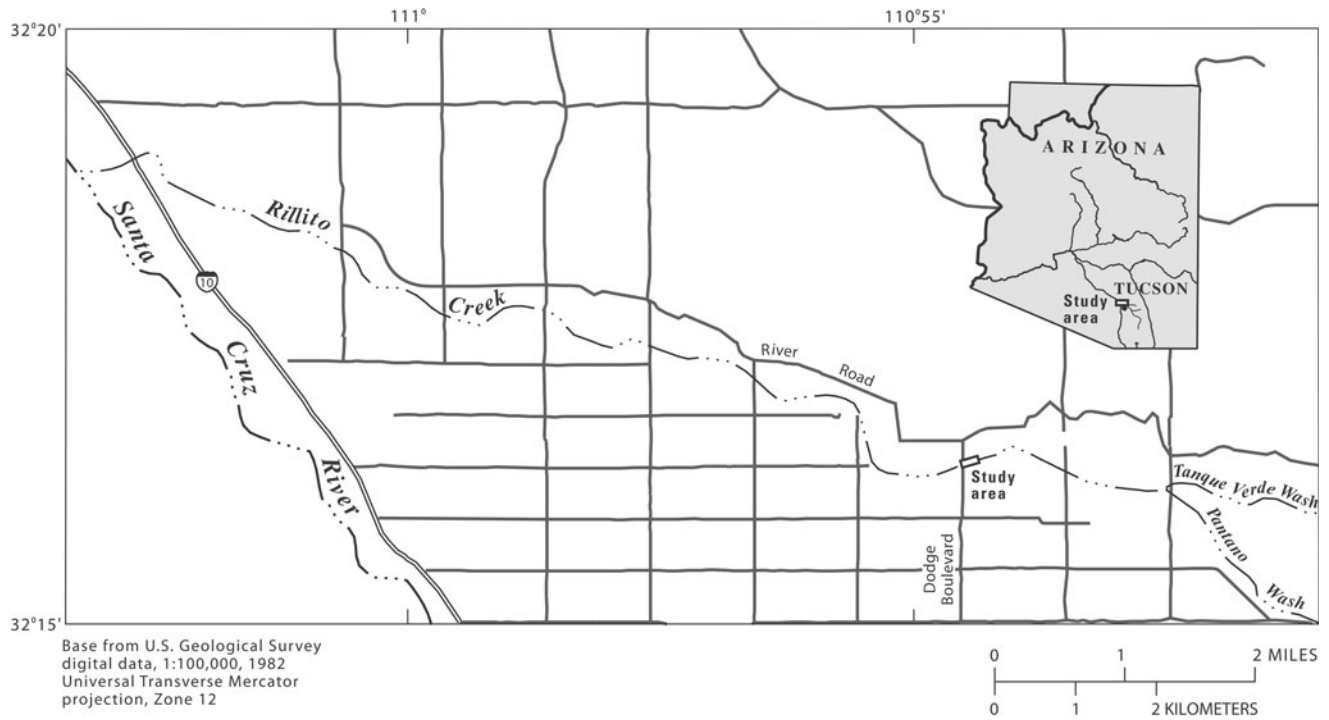


**Fig. 1** Location of Rillito Creek study area and view of Rillito Creek within the Tucson Basin, Tucson, Arizona. Photograph and schematic of the two-dimensional array of sensors within the stream channel deposits. Each *solid circle* represents a temperature and soil-water content sensor

161 flow events before monitoring began scoured 0.25 m from  
 162 the streambed surface. Subsequent scour and deposition  
 163 resulted in streambed elevation changes of less than 0.1 m.

Therefore, the measurement depths during the monitoring  
 period were 0.25, 0.50, 0.75, 1.0, 1.25, 1.75, and 2.25 m  
 below the streambed.

164  
 165  
 166

**Table 1** Soil hydraulic properties (mean and ranges) and top depths of the upper layer stream channel deposits and lower layer basin-fill deposits based on laboratory analyses of core samples and calibration of a variably saturated numerical model to observed drainage responses

| Layer                  | Number of samples | $\theta_r$ (cm <sup>3</sup> /cm <sup>3</sup> ) | $\theta_s$ (cm <sup>3</sup> /cm <sup>3</sup> ) | $\alpha$ (1/cm) | $n$       | $K_s$ (cm/d) | Top depth (m) |
|------------------------|-------------------|--|--|-----------------|-----------|--------------|---------------|
| Upper layer: core      | 5                 | 0.055  | 0.33   | 0.071           | 1.27      | 220          | 0             |
|                        |                   | 0.028–0.124                                    | 0.23–0.47                                      | 0.004–0.012     | 1.21–1.34 | 208–242      |               |
| Lower layer: core      | 8                 | 0.047  | 0.32   | 0.042           | 1.34      | 40           | 7             |
|                        |                   | 0.027–0.060                                    | 0.24–0.39                                      | 0.019–0.066     | 1.30–1.38 | 7–70         |               |
| Upper layer: simulated |                   | 0.06   | 0.33   | 0.07            | 1.5       | 600          | 0             |
| Lower layer: simulated |                   | 0.05   | 0.32   | 0.04            | 1.56      | 5            | 7             |

Residual soil moisture,  $\theta_r$ , and saturated soil moisture,  $\theta_s$ , van Genuchten parameters,  $\alpha$  (approximate of inverse of air entry) and  $n$  (slope of the retention function), and saturated hydraulic conductivity,  $K_s$

167 Soil moisture was measured with time domain reflectometry (TDR) every 2 min at each measurement depth.  
 168 Two-rod TDR probes were constructed using 0.32-cm-diameter stainless steel wave-guides, 0.2 m long and, spaced  
 169 0.03 m apart. To minimize signal transmission losses, RG-8 coaxial cable in lengths that ranged from 11 to 26 m was  
 170 used to connect the probes to the TDR instrument. A Campbell Scientific TDR100<sup>1</sup> (Campbell Scientific, Inc.,  
 171 Logan, UT) was used to transmit, receive, and convert waveforms into volumetric water content. TDR assemblies  
 172 were calibrated using Win TDR to determine the effective length of the cable and probe components. The effective  
 173 lengths of the probe and cable assemblies ascertained through laboratory calibration were used to infer volumetric  
 174 water content from the TDR100 responses. In addition, stream water temperature was measured using a TidbiT  
 175 thermistor (Onset Computer Corp., Bourne, MA) with a precision of 0.1°C, positioned at the bed sediment surface,  
 176 and located about 45 m downstream of the profiles. This thermistor was installed beneath a bridge and approximately  
 177 4 cm above the streambed surface.

188 **2 Results and discussion**

189 Data were collected from July 2000 through December 2001:  
 190 26 different streamflow events were recorded (Fig. 2). These  
 191 events varied in duration from 2 h to 11.6 days—16 events  
 192 were less than 1 day in duration, and only 3 events were longer  
 193 than 7 days. The median event lasted about 12 h. Peak discharge  
 194 for events ranged from 0.03 to 180 m<sup>3</sup>/s; the median discharge  
 195 was 3 m<sup>3</sup>/s. The no-flow period between flow events ranged from 6 h to 67 days. Water level measurements  
 196 from nested piezometers within the study area show that the  
 197 wetting front did not connect with the regional water table during any of the flow events. Of the 26 events, only 12 events  
 198 exhibited drainage at the 1.75 or 2.25 m depths before the  
 200

<sup>1</sup> Does not constitute endorsement by the U.S. Geological Survey.

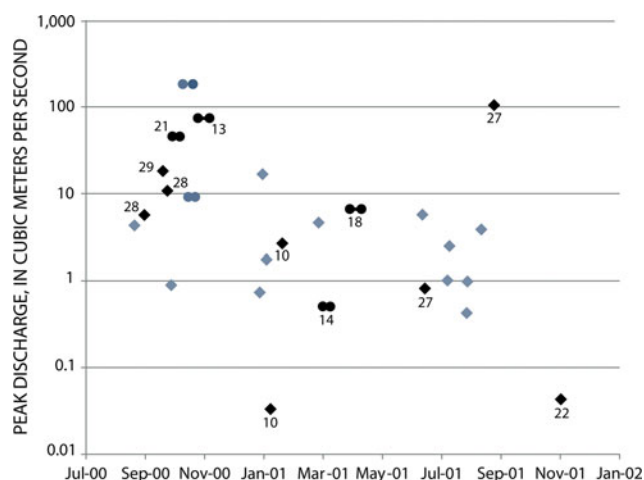


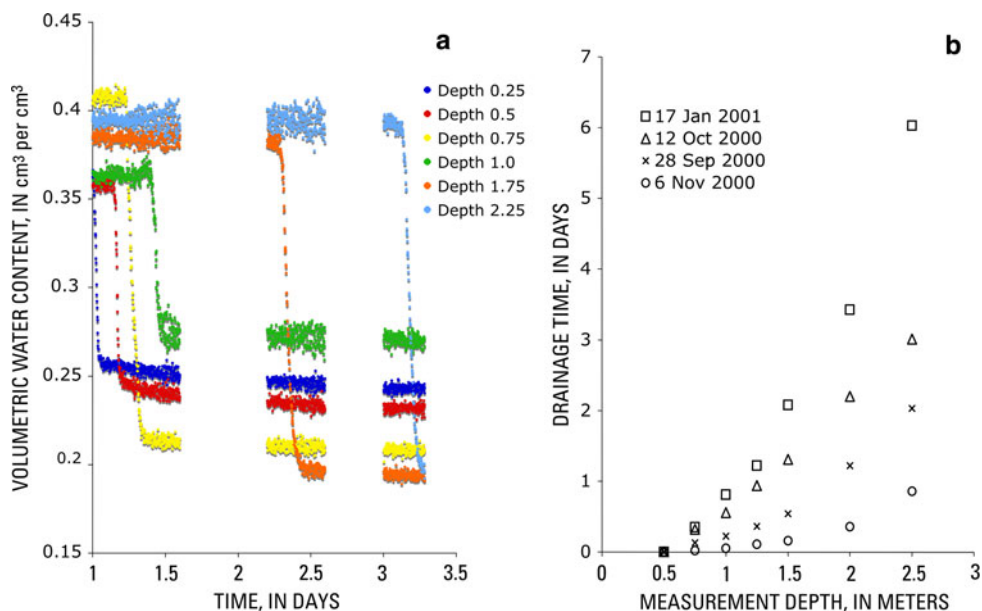
**Fig. 2** Hydrograph for Rillito Creek at Dodge Boulevard. Diamonds represent events that are less than 24 h in duration. Events are shown with their peak discharge value. Black symbols represent events that were used for the analysis. Numbers beside the black symbols represent the average temperature of the trench at the onset of the ephemeral event in degrees Celsius

onset of succeeding events. These 12 events were used in the  
 succeeding analysis. Multiple sensor profiles were used for  
 each of the events to provide 26 estimates of one-dimensional  
 vertical flow during and after streamflow.

2.1 Characteristic redistribution response

All of the drainage events showed similar characteristic  
 water content changes with time. As an example, one representative  
 event (September 10, 2000) is shown in Fig. 3a. The saturated  
 water content varied with depth between 0.35 and 0.42 cm<sup>3</sup>/cm<sup>3</sup>.  
 After approximately 2 days of drainage, the water content ( $\theta$ )  
 reached a near constant value at each depth. We refer to this as  
 the field capacity, and it ranged from  $\theta = 0.19$  to 0.27 cm<sup>3</sup>/cm<sup>3</sup>.  
 Drainage from full saturation to field capacity occurred very  
 rapidly at each depth, but there was a delay in the time of onset  
 of drainage with increasing depth.

**Fig. 3 a** Volumetric water content measurements ( $\text{cm}^3/\text{cm}^3$ ) at 6 depths (m) during drainage and **b** elapsed time (days) for the drainage front (defined as a volumetric water content of  $0.30 \text{ cm}^3/\text{cm}^3$ ) to travel from 0.25 m to each measurement depth for four flow events. Data gaps in Fig. 3a are a result of equipment malfunctions



217 For the observed soil moisture time series, the timing of  
 218 the onset of drainage at each measurement depth can be  
 219 described simply by the time that the water content  
 220 decreases below some water content threshold at that par-  
 221 ticular depth. We chose a water content value of  $0.30 \text{ m}^3/\text{m}^3$   
 222 as the threshold. Thus drainage for each depth began when  
 223 the soil moisture sensor measured  $0.30 \text{ m}^3/\text{m}^3$  and drainage  
 224 ended when the sensor measured field capacity. Given the  
 225 very rapid drainage response at each depth, the results  
 226 presented herein are not very sensitive to the specific value  
 227 of the threshold water content. Furthermore, because the  
 228 water content typically decreases from full saturation to this  
 229 threshold value within a few measurements, the results will  
 230 be insensitive to “smearing” due to the distributed spatial  
 231 sensitivity of the TDR probes (Ferré et al. 2002). Similarly,  
 232 errors in the specific calibration of dielectric permittivity to  
 233 water content relationship are not important for our analysis  
 234 given the rapid and large change in water content at the  
 235 onset of drainage.

236 Our shallowest measurement depth was 0.25 m, so we  
 237 have no information regarding the time required for the  
 238 drainage front to reach 0.25 m from the streambed surface.  
 239 We therefore calculated the elapsed time for drainage after  
 240 flow cessation at each depth as the difference between the  
 241 time that the threshold ( $0.30 \text{ m}^3/\text{m}^3$ ) was crossed for each  
 242 depth and the time that threshold was crossed at the shall-  
 243 est measurement depth, 0.25 m. Despite the similarity of  
 244 the drainage patterns among flow events, there were sig-  
 245 nificant variations in the absolute timing of drainage among  
 246 events (Fig. 3b). Additionally, there is some nonlinearity in  
 247 the velocity with depth (Fig. 3b). For this study, we con-  
 248 sidered the elapsed time to 1.75 m depth.

Owing to the extensive data set available, we first con-  
 ducted a systematic search for correlations between  
 drainage velocity and all other measured data. Specifically,  
 drainage velocity was plotted as a function of duration of  
 streamflow (period of event), no-flow period (period of  
 time between events), streambed temperature, maximum  
 stage, and normalized antecedent water content. To allow  
 for comparison of the simulation results with the mea-  
 surements in the field, the observed soil moisture data were  
 normalized such that each layer had normalized saturated  
 soil moisture,  $\theta_s$ , and residual soil moisture,  $\theta_r$ , values of  
 0.33 and 0.05, respectively:

$$\theta = 0.05 + \frac{\theta_{\text{meas}} - 0.05}{0.33 - 0.05}(\theta_{\text{max}} - 0.05)$$

where  $\theta$  is the normalized water content,  $\theta_{\text{meas}}$  is the  
 measured water content at each observation depth, and  
 $\theta_{\text{max}}$  is the maximum measured soil moisture value at that  
 same depth.

Temperature shows a strong linear correlation with the  
 measured drainage velocity (Fig. 4a). Linear regression to  
 temperature explains 87% of the observed variation in  
 elapsed drainage time to 1.75 m depth (Table 2). To see  
 whether this correlation can be further enhanced, we per-  
 formed partial least squares regression of all combinations  
 of the five measured variables to the elapsed time for  
 drainage. A linear combination of temperature and no-flow  
 period was shown to explain approximately 92% of the  
 measured variation in drainage velocity (Fig. 4f). No other  
 combination of two variables existed that exhibited such a  
 high correlation with the measured drainage velocities. We  
 initially concluded, based on the correlative analysis, that

**Fig. 4** Drainage time in days from 0.25 to 1.75 m as a function of **a** temperature, **b** length of no-flow, **c** duration of event, **d** maximum stage, and **e** normalized antecedent water content. **f** Predicted drainage times based on linear regression compared to measured drainage times as a function of  $T$  (temperature) and  $T$  and  $t_i$  (length of no-flow) combined

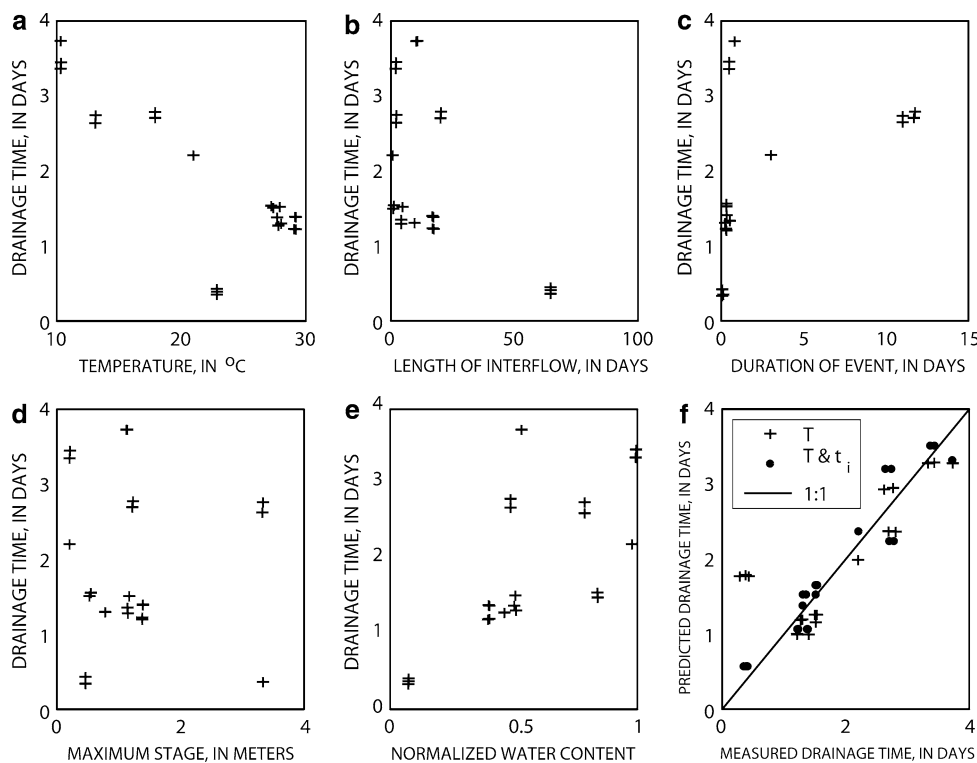


**Table 2** Correlative relationship between drainage velocity (m/days) and environmental controls for ephemeral streamflow drainage in Rillito Creek

|                            | Drainage velocity (m/days) | Temperature (°C) | No-flow period (days) | Event duration (days) | Maximum stage (m) |
|----------------------------|----------------------------|------------------|-----------------------|-----------------------|-------------------|
| Drainage velocity (m/days) | 1.00                       |                  |                       |                       |                   |
| Temperature (°C)           | -0.87                      | 1.00             |                       |                       |                   |
| No-flow period (days)      | -0.49                      | 0.14             | 1.00                  |                       |                   |
| Event duration (days)      | 0.51                       | -0.39            | -0.12                 | 1.00                  |                   |
| Maximum stage (m)          | 0.26                       | -0.22            | -0.17                 | 0.65                  | 1.00              |
| Normalized water content   | 0.56                       | -0.38            | -0.81                 | 0.15                  | -0.05             |

279 water temperature exerts a primary control on drainage rate  
 280 in Rillito Creek and that the duration of the no-flow period  
 281 has a smaller, secondary impact, probably through its impact  
 282 on the initial water content throughout the profile. This is  
 283 evidenced through the strong correlative relationship  
 284 between antecedent normalized water content and the no-  
 285 flow period (Table 2). These results seemed appropriate as  
 286 higher temperatures produce larger hydraulic conductivities  
 287 and higher drainage velocities. This is consistent with, for  
 288 instance, the Jury and Horton (2004) rectangular drainage  
 289 model, which would show faster drainage with higher  $K_{sat}$ .

290 **2.2 Parameter estimation for a base case flow event**

291 Correlative models are used widely in hydrologic sciences  
 292 due to their computational efficiency and their ability to

293 assimilate data continuously (e.g. Modarres 2007; Ramos 293  
 294 2006). Some of these models are based purely on correlation 294  
 295 while others make an explicit effort to link the correlative 295  
 296 relationships to more complex and computationally intensive 296  
 297 physical models (e.g. Gau et al. 2006). One clear danger of 297  
 298 correlation-based approaches is that observations may be 298  
 299 correlated with other, unmeasured states, leading to incor- 299  
 300 rect assumptions regarding causation. In contrast, while 300  
 301 physical models are better able to identify sensitivities to 301  
 302 and interactions among parameters, and therefore to identify 302  
 303 causation, they are susceptible to errors due to the exclu- 303  
 304 sion of important processes during model conceptualization. 304  
 305 This has led to recent efforts to formalize the process of 305  
 306 model conceptualization (e.g. Sivakumar 2008). In the context 306  
 307 of this study, a colleague (Shlomo Neuman, personal commu- 307  
 308 nication) pointed out that correlation-based 308

309 findings need to be supported by a physical model to ensure  
310 the purported interactions among environmental controls on  
311 drainage are reasonable. So, we decided to test our initial  
312 conclusions with a physically-based variably saturated  
313 numerical flow model.

314 Given the similarity in responses among the four later-  
315 ally separated columns of sensors, water flow was assumed  
316 to be vertical during drainage. HYDRUS-1D (Simunek  
317 et al. 1999) was used to simulate infiltration and drainage.  
318 On the basis of core data, the subsurface was comprised of  
319 two layers (Table 1): a shallow streambed layer and an  
320 underlying basin fill layer. Therefore, although all of our  
321 measurements are located in the upper layer, we modeled  
322 the system using two layers, with a contact below our  
323 deepest measurement point.

324 One flow event was chosen as a base case: 12 October,  
325 2000. This event was selected because it had intermediate  
326 values of temperature (21°C), flow duration (3 days), and  
327 elapsed time to 1.75 m (2.2 days) of the drainage front  
328 from 0.25 to 1.75 m depth. This allowed us to do single  
329 parameter sensitivity analyses, both increasing and  
330 decreasing each parameter, and then to compare the pre-  
331 dicted and observed drainage velocities over the observed  
332 range of environmental conditions. The measured water  
333 content before the base case flow event began was about  
334  $0.29 \text{ cm}^3/\text{cm}^3$ . The normalized antecedent water content  
335 for the base case event was  $0.26 \text{ cm}^3/\text{cm}^3$  throughout the  
336 entire profile.

337 The first step was to adopt the soil hydraulic properties  
338 measured on core samples collected near the site (Table 1)  
339 together with the measured flow duration, antecedent water  
340 content, and antecedent water temperatures measured in the  
341 stream and within the soil matrix at each depth. Initially, the  
342 upper boundary was represented as a zero pressure head  
343 during flow and with a temperature equal to that of the  
344 stream water. Drainage was modeled with a zero flux top  
345 boundary and temperatures within the model domain equal  
346 to the antecedent temperatures. The upper boundary tem-  
347 peratures did not vary. To facilitate convergence of HY-  
348 DRUS-1D with the recommended settings of the Picard  
349 numerical solution scheme, the van Genuchten  $n$  values  
350 were increased for both layers from their core-derived  
351 values (Table 1). All other soil hydraulic parameter values  
352 and environmental conditions were kept to their measured  
353 values. The model-predicted drainage behavior (Fig. 5a)  
354 was quite different from that observed in the field (Fig. 3a).  
355 Specifically, the simulated response did not show the  
356 characteristic rapid drainage at each depth with delays  
357 among depths seen in the field data. The model-predicted  
358 elapsed time to each measurement depth did not agree with  
359 the observations, either (Fig. 5b). The core-derived  
360 parameters were obtained from a well drilled in a small  
361 bench next to the stream channel. The bench appeared to

362 have a higher content of fines than the coarse alluvium of  
363 the stream channel. Thus we considered that the upper layer  
364 hydraulic conductivity values from the bench may be lower  
365 than those in the stream channel. Hydraulic conductivities  
366 of the lower layer were assumed to be the similar between  
367 the well cores and layers underlying the trench.

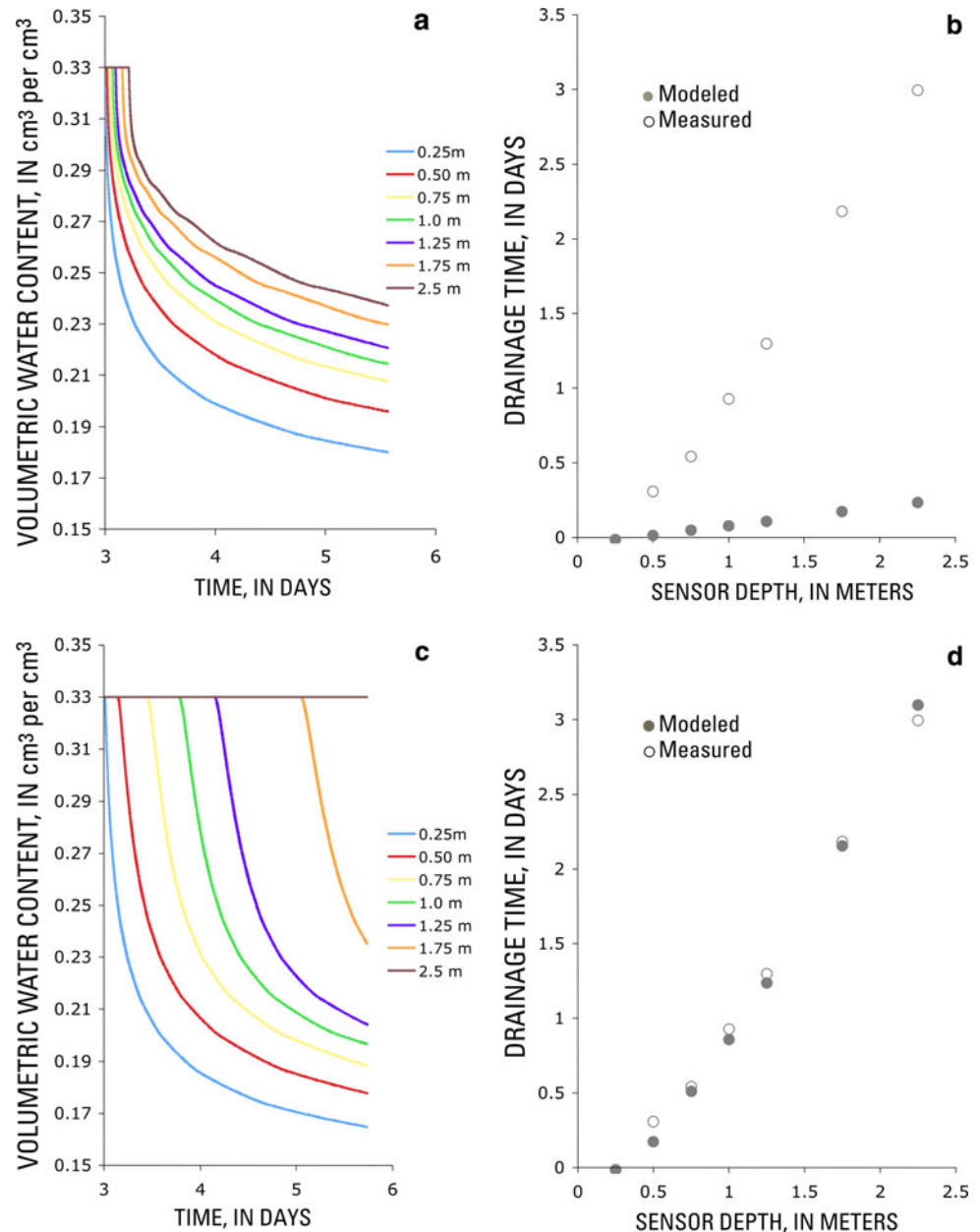
368 Because the independently measured soil hydraulic  
369 properties did not predict the observed drainage behavior,  
370 we attempted to estimate the parameter values based on  
371 drainage velocity observations. For simplicity, hydraulic  
372 parameter values were varied manually to improve the fit to  
373 the observed elapsed times for the representative base case.  
374 During this manual parameter estimation, we kept as many  
375 of the measured core-based parameter values and environ-  
376 mental conditions equal to their measured value as possible.  
377 Indeed, we could fit the soil moisture observations reason-  
378 ably well (Fig. 5c) by changing only the hydraulic con-  
379 ductivities of the two soil layers (Table 1). Specifically, we  
380 had to reduce the hydraulic conductivity of the lower layer  
381 to 5 cm/day to match the delay in drainage among the  
382 different measurement depths. This inferred value is similar  
383 to the lowest core-measured value of 7 cm/day. The  
384 hydraulic conductivity of the upper layer was increased to  
385 three times the highest core measurement to produce the  
386 rapid drainage observed at each measurement depth. The fit  
387 between the simulated and measured elapsed time to 1.75-m  
388 depth can also be considered reasonable (Fig. 5d). No for-  
389 mal estimation of parameter uncertainty was conducted for  
390 this analysis because our objective was to test the validity of  
391 our conceptual model of temperature dependent drainage,  
392 rather than to determine the soil hydraulic parameter values  
393 for predictive modeling.

### 2.3 Hypothesis testing: dependence of drainage velocity on temperature

394  
395  
396 Having matched the base case response, the manually  
397 calibrated HYDRUS-1D model was used to examine the  
398 dependence of drainage velocity on temperature, flow  
399 duration, and normalized antecedent water content. With  
400 our event-based modeling approach, we could not examine  
401 the impacts of changes in the no-flow period. For the  
402 remaining four variables (temperature, duration of event,  
403 maximum stage, and normalized antecedent water content),  
404 each parameter value was varied over its observed range  
405 while maintaining the values of all other base case  
406 parameters and environmental conditions.

407 Results from the single parameter manual sensitivity  
408 analysis indicate that the observed temperature variations  
409 cannot explain the observed range of variation of the  
410 drainage velocity (Fig. 6a). Specifically, despite the strong  
411 correlation between drainage velocity and temperature  
412 observed in the field data (Fig. 4) the numerical model

**Fig. 5** **a** Simulated water content ( $\text{cm}^3/\text{cm}^3$ ) at each measurement depth based on core-derived parameters; **b** measured and simulated elapsed time (days) for the drainage front (defined as a volumetric water content of  $0.30 \text{ cm}^3/\text{cm}^3$ ) to reach each measurement depth based on core-derived parameters; **c** simulated water content ( $\text{cm}^3/\text{cm}^3$ ) at each measurement depth using calibrated parameters; and **d** measured and simulated elapsed time (days) for the wetting front to reach each measurement depth based on calibrated parameters

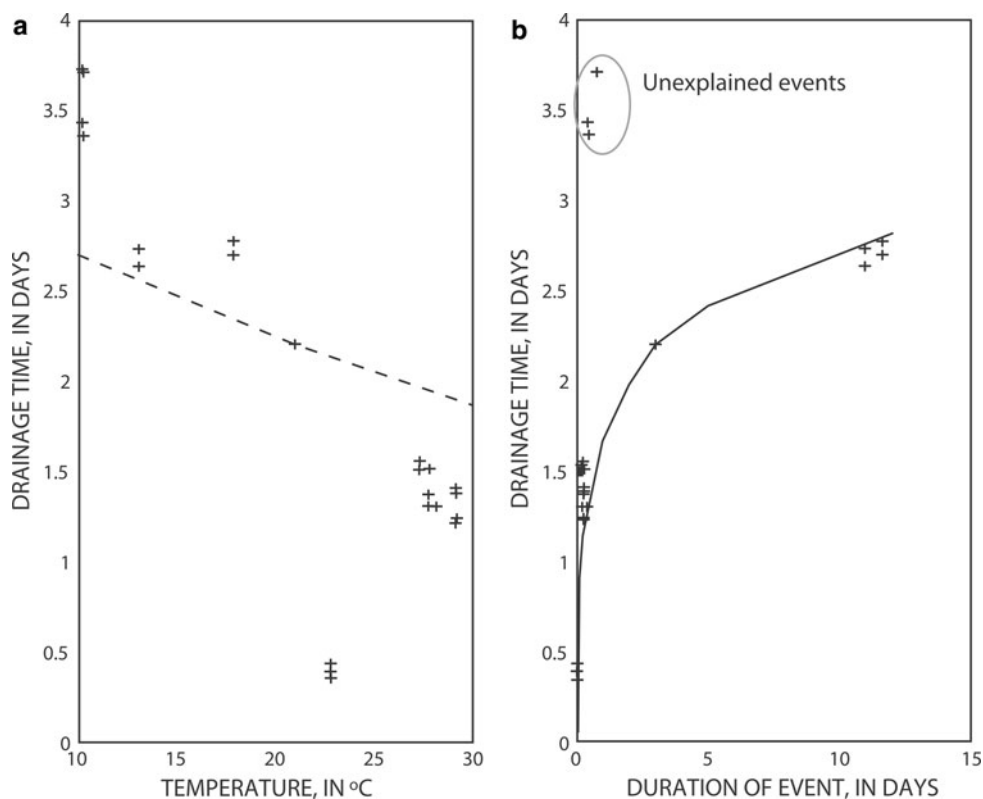


413 contradicted our initial conclusion that water temperature is  
414 a primary control on drainage velocity.

415 Having disproven our initial, data-driven primary  
416 hypothesis, other possible physical causes for the changes in  
417 drainage velocity were considered. Antecedent water content  
418 was evaluated because it can control the capillary gradient  
419 at the wetting front during drainage. Specifically,  
420 higher initial water contents would result in decreased  
421 capillary gradients across the wetting front, thereby slowing  
422 drainage. This assumes that increases in unsaturated  
423 hydraulic conductivity from higher initial water contents  
424 are small compared to the range in conductivities caused by  
425 capillary gradients. However, similar to the results for water

426 temperature, variations in antecedent water content within  
427 the numerical model could not explain the observed variations  
428 in drainage velocity (not shown). Next, the duration of  
429 flow was evaluated. Flow duration contributes to wetting  
430 front depth at the end of the flow event and, thereby, the  
431 contribution of capillarity to the drainage response. Specifically,  
432 shorter flow duration would result in a larger capillary gradient  
433 from the ground surface across the wetting front, leading to faster  
434 drainage. In fact, the modeling results support this interpretation:  
435 the observed range of variations in flow duration explains most of  
436 the observed variation in drainage velocity (Fig. 6b). Only two flow  
437 events with short flood durations and long drainage times  
438

**Fig. 6** Simulated drainage time from 0.25 to 1.75 m as a function of **a** temperature and **b** length of event. Drainage was simulated using a two-layer, one-dimensional flow model, HYDRUS 2-D (Simunek et al. 1999). The model was calibrated to the flow event with a temperature of 21°C and a duration of 3.3 days. The temperature and then the duration of event were varied while all other parameters were held constant to produce the results shown by the *dashed* (temperature) and *solid* (duration of event) shown. Crosses represent the observed data



439 could not be explained using the calibrated model. This  
440 suggests that there is at least one other process that is not  
441 considered in our conceptual model.

#### 442 2.4 Comparing correlation-based and physically-based 443 data analysis approaches

444 The correlation-based approach to data analysis suggested  
445 that the drainage response was primarily controlled by  
446 temperature, with a secondary dependence on no-flow  
447 period. In this case, the rapid drainage events that are not  
448 explained by a linear dependence on temperature are  
449 associated with the longest no-flow periods (Fig. 4e and b).  
450 This could suggest that something related to long no-flow  
451 periods has a strong influence on the drainage responses.  
452 But, closer inspection suggests that the result may be an  
453 artifact of the partial least squares regression approach and  
454 the assumption of a linear relationship. Specifically, the  
455 drainage times that are not explained by temperature have  
456 no-flow periods that are far longer than the other flow  
457 events (Fig. 4b). Therefore, including no-flow period in a  
458 multiple linear regression can change the predicted  
459 response for the outlying events (where no-flow period has  
460 large leverage) while having very little impact on the  
461 predictions for the events that are explained by a linear  
462 temperature dependence (where no-flow period has very  
463 small leverage).

More critically, HYDRUS-1D showed that the slope of  
the dependence of drainage velocity on temperature that is  
evident in the data is not consistent with the physical  
dependence of drainage on temperature. In fact, in Tucson,  
winter flows are characterized by cold water temperatures  
and longer durations; whereas summer flows have warm  
water temperatures and shorter durations. Therefore, much  
of the apparent dependence of drainage velocity on tem-  
perature may actually be due to correlation of temperature  
with flow duration. This points out a critical limitation to  
correlation-based analysis: unrecognized relationships,  
primarily nonlinear in nature, between variables can result  
in misinterpretation of causative relationships.

Sensitivity analysis using HYDRUS-1D suggests  
strongly that flow duration controls the drainage response  
for all but a few events (Fig. 6b). Longer duration flow  
events resulted in a decreased drainage rate. In general,  
capillary gradients in the subsurface profile exhibit the  
greatest influence on drainage at the cessation of flow. Thus  
a longer duration event with a large infiltration of water into  
the subsurface reduces the capillary gradients. The larger  
infiltration of water can result from ephemeral events  
characterized by low antecedent water contents, high stage,  
high temperatures, and longer duration. However, the  
greatest volumes of water transmitted to the sediment pro-  
file occur with duration. While temperatures from infil-  
trating water can persist in the subsurface after the cessa-  
tion

|     |   |  |     |
|-----|---|--|-----|
| 491 | of streamflow the depth of influence is limited to the  | variables no matter how minor the relationship determined      | 544 |
| 492 | upper sediments and magnitude of impact decreases with  | by the preconceived conceptual model.                          | 545 |
| 493 | time.   |  |     |
| 494 | This physically-based analysis leads to more convincing   | 2.5 Implications of correlation- and physically-based          | 546 |
| 495 | explanations of drainage behavior for most of the flow  | analyses for water management                                  | 547 |
| 496 | events, and only two events (Jan 16, 2001; Jan 27, 2001)  |  |     |
| 497 | are not explained using this analysis. These two unex-  | In a managed stream reach, optimal water availability in       | 548 |
| 498 | plained events had a confounding impact on the results of   | the rhizosphere can be adjusted to match the requirements      | 549 |
| 499 | the correlative analysis. The two unexplained events had  | of the local riparian vegetation (Leenhouts et al. 2006;       | 550 |
| 500 | the lowest water temperatures (10.3°C, 10.3°C), relatively  | Stromberg et al. 2007). Results of our physically-based        | 551 |
| 501 | short no-flow (2.6 days, 10.6 days) and flow durations  | analysis suggest that for Rillito Creek and other similar      | 552 |
| 502 | (0.49 days, 0.82 days), relatively low stage (6.7 cm,   | environments the length of flow should be adjusted to          | 553 |
| 503 | 34.4 cm) and intermediate antecedent water contents   | control the length of time that water will be available to     | 554 |
| 504 | (0.29 cm <sup>3</sup> /cm <sup>3</sup> , 0.22 cm <sup>3</sup> /cm <sup>3</sup> ). These drainage events | plants after a flow event. In contrast, the correlation-based  | 555 |
| 505 | occurred during and after five consecutive flow events from   | analysis suggested that water temperature is the primary       | 556 |
| 506 | January 8 through 27, 2001. The two outlying events (each   | control variable. The inconsistency is related to the corre-   | 557 |
| 507 | with two profiles) are labeled on Fig. 5b. It is suggested  | lation between temperature and event durations as well as      | 558 |
| 508 | that the consecutive events prior to these two events could   | the use of a tool that may not discern nonlinear relation-     | 559 |
| 509 | be acting as a single long duration event and thus ante-  | ships. These differing interpretations between numerical       | 560 |
| 510 | cedent conditions in the water profile are not accurately   | modeling and correlative analysis could have significantly     | 561 |
| 511 | represented. Even considering the multiple short duration   | different implications for water resources management          | 562 |
| 512 | events as a single event does not account for the drainage  | practices, especially for assessing the relative risks of dif- | 563 |
| 513 | rate. Future research should focus especially on drainage   | ferent approaches for controlled release of water into         | 564 |
| 514 | following successive cold flow events or, perhaps, on   | ephemeral channels, construction of detention facilities, or   | 565 |
| 515 | identifying other properties that were not measured that  | other channel adjustment features (restorative or artificial). | 566 |
| 516 | could explain these two responses.  |  |     |
| 517 | Our initial conceptual model was based on standard  | <b>3 Conclusions</b>   | 567 |
| 518 | treatments of one-dimensional infiltration and drainage in a  |  |     |
| 519 | homogeneous porous medium. Solutions such as those  | As is the case for many ephemeral channels in alluvial         | 568 |
| 520 | presented by Philip (1957) suggest that infiltration will be  | aquifer systems, the hydrogeology of Rillito Creek consists    | 569 |
| 521 | high at early stage of wetting and will reduce with time as   | of a coarse-grained highly permeable alluvial layer over-      | 570 |
| 522 | the contribution of sorptivity decreases. Similarly, simple   | lying a finer-grained and less permeable basin-fill layer.     | 571 |
| 523 | drainage models, such as the rectangular drainage model   | We observed a distinctive drainage response following          | 572 |
| 524 | presented by Jury and Horton (2004) suggest that the  | many flow events, with a sharp drainage front advancing        | 573 |
| 525 | wetting front velocity will decrease with time as the profile   | downward with time. This response has significant impacts      | 574 |
| 526 | drains. For the flow events observed during this investi-   | on the availability of water to near- and in-channel vege-     | 575 |
| 527 | gation, we expected infiltration would be dominated by  | tation. A physically based one-dimensional numerical flow      | 576 |
| 528 | gravity and that drainage would be dominated by the   | model replicated this response for all but two events. The     | 577 |
| 529 | hydraulic properties of the medium that control the   | hydraulic parameters inferred from the model fits and from     | 578 |
| 530 | hydraulic conductivity. Our initial conceptual model was  | cores are similar to those measured in other ephemeral         | 579 |
| 531 | further influenced by the data we had available. As is  | streams (Coes and Pool 2005), suggesting that the observed     | 580 |
| 532 | commonly the case with correlative approaches, we sought  | drainage pattern is not specific to the Rillito Creek, but may | 581 |
| 533 | explanations of our observed behavior (drainage velocity)   | occur in many ephemeral channels.                              | 582 |
| 534 | based on our available data (water temperature and water  | The observed drainage front velocity showed a clear            | 583 |
| 535 | content in the shallow sediments with time). In retrospect,   | linear correlation with water temperature. Partial least       | 584 |
| 536 | it is clear that the correlative approach was misleading  | squares regression analysis suggested that temperature and     | 585 |
| 537 | because flow duration and water temperature were highly   | the duration of the no-flow period preceding the monitored     | 586 |
| 538 | correlated. But, neither our initial conceptual model nor our   | drainage event could explain more than 90% of the vari-        | 587 |
| 539 | available data and linear correlative analysis suggested  | ability in observed drainage velocity. However, numerical      | 588 |
| 540 | flow duration as a primary control on drainage velocity.  | water flow simulations showed that the measured variations     | 589 |
| 541 | Thus, an additional, although basic point, is that the inde-  | in soil temperature cannot explain the observed variations     | 590 |
| 542 | pendency of relationships between interrogated variables is   | in drainage velocity. Rather, the physically-based model       | 591 |
| 543 | important to consider when investigating regressions of   |  |     |

592 indicated that the duration of the flow event preceding the  
593 monitored drainage event is most important in determining  
594 drainage velocity. Capillary gradients in the subsurface  
595 profile exhibit the greatest influence on drainage at the  
596 cessation of flow. Thus a longer duration event with a large  
597 infiltration of water into the subsurface reduces capillary  
598 gradients.

599 In summary, this work provides two important conclu-  
600 sions. First, this study presents a simple, yet powerful  
601 example of the potential pitfalls of depending solely upon  
602 correlative data analyses to understand or predict hydro-  
603 logic processes. Second, the dependence of drainage  
604 velocity on event duration has direct implications for the  
605 time that water is available for use by plants in ephemeral  
606 channels and for the assessment of alternative approaches  
607 for stream restoration.

608 **Acknowledgments** We would like to thank Shlomo Neuman for  
609 discussions that established the need for numerical modeling beyond  
610 simple correlative data analysis and the USGS Arizona Water Science  
611 Center for its financial support. The 3rd author was supported by a  
612 J. Robert Oppenheimer Fellowship from the LANL postdoctoral  
613 program.

## 614 References

- 615 Bendix J, Hupp CR (2000) Hydrological and geomorphological  
616 impacts on riparian plant communities. *Hydrolog Process*  
617 14:2977–2990
- 618 Blasch K (2003) Streamflow timing and estimation of infiltration rates  
619 in and ephemeral stream channel using variably saturated heat  
620 and fluid transport methods, Ph.D. Dissertation, University of  
621 Arizona, Tucson, 204 p
- 622 Coes AL, Pool DR (2005) Ephemeral-stream channel and basin-floor  
623 infiltration and recharge in the Sierra Vista subwatershed of the  
624 Upper San Pedro Basin, southeastern Arizona: U.S. Geological  
625 Survey Open-File Report 2005-1023, 67 p
- 626 Constantz J (1998) Interaction between stream temperature, stream-  
627 flow, and groundwater exchanges in alpine streams. *Water*  
628 *Resour Res* 34(7):1609–1615
- 629 Davidson ES (1973) Geohydrology and water resources of the Tucson  
630 basin, Arizona: U.S. Geological Survey Water-Supply Paper  
631 1939-E, 81 pp
- 632 Ferré TPA, Nissen HH, Simunek J (2002) The effect of the spatial  
633 sensitivity of TDR on inferring soil hydraulic properties from  
634 water content measurements made during the advance of a  
635 wetting front. *Vadose Zone J* 1:281–288

- Gau HS, Hsieh CY, Liu CW (2006) Application of grey correlation  
636 method to evaluate potential groundwater recharge sites. *Stoch*  
637 *Environ Res Risk Assess* 20:407–421
- Hoffmann JP, Ripich MA, Ellett KE (2002) Characteristics of shallow  
639 deposits beneath Rillito Creek, Pima County, Arizona, U.S.  
640 Geological Survey Water-Resources Investigations Report 01-  
641 4257, 51 pp
- Hupp CR, Osterkamp WR (1996) Riparian vegetation and fluvial  
643 geomorphic processes. *Geomorphology* 14:277–295
- Jury WA, Horton R (2004) Soil physics, 6th edn. Wiley, Hoboken,  
645 NJ, 370 pp
- Leenhouts JM, Stromberg JC, Scott RL (eds) (2006) Hydrologic  
647 requirements of and consumptive ground-water use by riparian  
648 vegetation along the San Pedro River, Arizona, U.S. Geological  
649 Survey Scientific Investigations Report 2005–5163, 154 pp
- Loik ME, Breshears DD, Lauenroth WK, Belnap J (2001) A multi-  
651 scale perspective of water pulses in dryland ecosystems:  
652 climatology and ecohydrology of the western USA. *Oecologia*  
653 141:269–281. doi:10.1007/s00442-004-1570-y
- Lytle DA, Poff NL (100) 2004. Adaptations to natural flow regime  
655 TRENDS Ecol Evol(19):2–94
- Modarres R (2007) Streamflow drought time series forecasting. *Stoch*  
657 *Environ Res Risk Assess* 21:223–233
- Philip JR (1957) The theory of infiltration: 1. The infiltration equation  
659 and its solution. *Soil Sci* 83:345–357
- Ramos JA (2006) Exponential data fitting applied to infiltration,  
661 hydrograph separation, and variogram fitting. *Stoch Environ Res*  
662 *Risk Assess* 20:33–52
- Shaw RS, Cooper DJ (2008) Linkages among watersheds, stream  
664 reaches, and riparian vegetation in dryland ephemeral stream  
665 networks. *J Hydrol* 350:68–82
- Simunek J, Sejna M, van Genuchten MT (1999) The HYDRUS-1D  
667 software package for simulating two-dimensional movement of  
668 water, heat, and multiple solutes in variably-saturated media,  
669 version 2.0. IGWMC-TPS-53, 251 pp., Int. Ground Water  
670 Modeling Cent., Colo. Sch. of Mines, Golden, Colo
- Sivakumar B (2008) Dominant processes concept, model simplification  
672 and classification framework in catchment hydrology. *Stoch*  
673 *Environ Res Risk Assess* 22:737–748
- Stonstrom DA, Constantz J, Ferré TPA, Leake SA (eds) (2007)  
675 Ground-water recharge in the arid and semi-arid southwestern  
676 United States: U.S. Geological Survey Professional Paper 1703,  
677 414 p
- Stromberg JC, Lite SJ, Marler R, Paradzick C, Shafroth PB, Shorrock  
679 D, White JM, White MS (2007) Altered stream-flow regimes and  
680 invasive plant species: the Tamarix Case. *Global Ecol Biogeogr*  
681 16:381–393
- Tadayon S, Duet NR, Fisk GG, McCormack HF, Partin CK, Pope GL,  
683 Rigas, PD (2001) Water resources data for Arizona, water year  
684 2000: U.S. Geological Survey Water-Data Report AZ-00-1,  
685 390 pp
- 687